Kaplan-Meier Type Estimators for Linear Contact Distributions

MARTIN B. HANSEN

The Royal Veterinary and Agricultural University, Copenhagen

RICHARD D. GILL

University of Utrecht

ADRIAN BADDELEY

University of Western Australia and University of Leiden

ABSTRACT. **The linear contact distribution function is shown to be continuously differentiable for any stationary random closed set, which implies the existence of a continuous density and hazard rate. Moreover, it is proved that the density is monotone decreasing. When the linear contact distribution function is estimated from observations in a bounded window, the distance to the set of interest from a fixed point in a given linear direction is right-censored by its distance to the boundary of the window. We develop a Kaplan-Meier type estimator for the linear contact distribution function and hazard rate. We show that the new estimator has a ratio-unbiasedness property and that it is an absolutely continuous distribution function. A CLT is derived for independent replications within a fixed observation window. The techniques are applied to the analysis of spatial patterns in acid milk. The feature of replication of the images and the CLT for the estimator give confidence bounds on the estimator. This is used to discriminate between different kinds of heat treatments.**

Key words: edge effects, linear first contact statistics, Kaplan-Meier estimator, random closed sets, reduced sample estimator, spatial statistics, protein network, hazard rate, stochastic geometry, Boolean model, star volume

1. Introduction

In this paper we use the linear contact distribution function to analyse binary patterns like those displayed in Fig. 1. These results are complementary to the work done for the empty space (spherical contact) distribution, for point processes in Baddeley and Gill (1993) and random closed sets in Baddeley and Gill (1994).

An important tool in the exploratory data analysis of random patterns is the distributions to first contact, for increasing test sets contained in the void. These functions give important properties of the "pore" space between particles. In the present paper the test set, normally called the structuring element, is chosen to be a line segment. Efficient estimation of the distribution to first contact has many applications in the analysis of spatial patterns (Serra, 1982); it enables e.g. "tests" for isotropy, because if isotropy is assumed, then the distribution is independent of the orientation of the line segment (Stoyan et al., 1987, Section 6.2). Perhaps more interestingly a similar approach may be used to estimate the preferred alignment of sets (Hall, 1988). Moreover, the 3-dimensional linear contact distribution can be estimated directly from 2-dimensional slices of the structure parallel to the orientation of the structuring element as the estimator does not require additional information from the "missing" dimension. Finally the linear contact distribution can be used to estimate parameters of specified spatial models (Cressie, 1991, Section 9.5).

However, the estimated function is normally greatly influenced by edge effects because the random set is observed in a bounded window. Essentially when a certain point x is used as a reference point, the information whether or not a grown test set centered at x touches the random set is censored by its grown distance to the boundary of the window.

The presence of censored observations in spatial data sets when estimating the distribution function at distance r, is normally dealt with by restricting attention to those points observed up to distance r without censoring, leading to what is called the reduced sample estimator (previous

literature have called it a variety of other names, e.g. the border method or minus sampling). Such an analysis will not usually utilize the data optimally. Methods for dealing with such incomplete observations have traditionally been developed for survival analysis, because similar censoring occurs in clinical investigations. The relation between censoring and spatial data was noted first by Laslett (1982) who observed that the lengths of the segments in a line process observed in a bounded window are censored. However, the connection between the Kaplan-Meier (1958) type estimator and censoring of survival time was quite surprisingly first noted recently by Baddeley and Gill (1993) for the empty space distribution of spatial point processes, and later developed for random closed sets in Baddeley and Gill (1994). The methods can largely be carried over to linear structuring elements.

The paper is organized as follows. Section 2 describes the data set to be analysed. In Section 3 some definitions from spatial statistics are recalled, the continuous differentiability of the linear contact distribution function is proved, connections to the rose of direction are outlined, and the behaviour of the linear contact function for the Boolean model is discussed. Methods for estimating the linear contact distribution function are discussed in Section 4, and the implementation of the estimation procedure is described in Section 5. Asymptotics and analysis of the data set are presented in Section 6. Finally the results obtained are discussed in Section 7.

2. The data set

Fig. 1. Fig. 1 shows four images of protein network in a yoghurt ferment, see Skriver et al. (1995). In the experiment two durations of pasteurization were carried out, 85C/20 min and 85C/30 min, to be called the "short" and "long" heat treatments, respectively. The samples were prepared by thin sectioning and images were obtained from a transmission electron microscope. At two different magnifications ($\times$5000 and $\times$7500) 12 pictures were taken from each experimental group. The images

were taken sufficiently far apart to assume "independence". The pictures were digitized by a CCD camera with 512×512 pixels. To avoid microscope marks a 500×500 sub image was extracted for further analysis. After segmentation by thresholding, the images were subjected to a morphological erosion and dilation. Finally irrelevant objects were deleted manually (fat particles, bacteria, etc.). For more details on the image processing see Skriver et al. (1995). Typical examples of the 48 images of the remaining network are shown in Fig. 1, one from each experimental group. The objectives of the investigation in Skriver et al. (1995) were

- to evaluate the use of digital image analysis techniques to quantify the texture in acid milk gels by quantitative parameters;
- to investigate the ability of image analysis to differentiate between electron microscope pictures with different duration of the heat treatment.

This was done by calculating basic stereological parameters, such as amount of protein, surface content, and by calculating the covariance function, star volume and scaling properties. In the present study we pursue these aims, with the use of the linear contact function, together with a development of the Kaplan-Meier technique (Baddeley and Gill, 1993) for estimation of hitting distributions with a linear structuring element.

3. The linear contact function F

3.1. Preliminaries from spatial statistics

3.1.1. Linear contact distribution

Let X be a stationary random closed set in $\mathbb{R}^k$ (Matheron, 1975), observed through a bounded window $W \subset \mathbb{R}^k$. The problem is, based on the observable data $X \cap W$, to estimate the function F

defined as follows. Let e be a unit vector in $\mathbb{R}^k$, and $B = \{te : -1 \leq t \leq 1\}$ a line segment of length 2. For $A, B \subset \mathbb{R}^k$, Minkowski addition $\oplus$ and subtraction $\ominus$ are defined by

$$\begin{aligned} A \oplus B &= \{x + y : x \in A, y \in B\} \\ A \ominus B &= (A^c \oplus B)^c. \end{aligned}$$

For $x \in \mathbb{R}^k$ we often write A_x instead of $A \oplus \{x\}$. Moreover, we define the symmetrical set of B and the scalar dilation of A by $r \in \mathbb{R}$, by putting

$$\begin{aligned} \check{B} &= \{-x : x \in B\} \\ rA &= \{rx : x \in A\}. \end{aligned}$$

Let

$$\rho_B(x, A) = \inf\{r \geq 0 : (rB)_x \cap A \neq \emptyset\}$$

Fig. 2.

be the "shortest" distance to A from x "looking both ways" along the directional vector e, see Fig. 2. By the definition of Minkowski addition and subtraction and assuming A to be closed it can be shown that

$$\begin{aligned} A \oplus r\check{B} &= \{x \in \mathbb{R}^k : \rho_B(x, A) \leq r\} \\ A \ominus r\check{B} &= \{x \in A : \rho_B(x, A^c) > r\}. \end{aligned}$$

However as B is assumed to be symmetrical we immediately get $B = \check{B}$ and therefore if A is closed

$$\begin{aligned} A \oplus rB &= \{x \in \mathbb{R}^k : \rho_B(x, A) \leq r\} \\ A \ominus rB &= \{x \in A : \rho_B(x, A^c) > r\}. \end{aligned}$$

Finally define the coverage fraction of X by $p_X = \mathbb{P}\{0 \in X\}$, and for $r \geq 0$ the linear contact function by

$$F(r) = \mathbb{P}\{\rho_B(0, X) \leq r\}.$$

With $|\cdot|_k$ denoting k-dimensional volume, and Z a measurable set with $|Z|_k > 0$, we will make use of a standard result in stochastic geometry (Robbins' Theorem (Robbins, 1944, 1945, 1947), originally proved in a special case by Kolmogorov (1992))

$$p_X = \frac{\mathbb{E}|Z \cap X|_k}{|Z|_k} = \mathbb{P}\{0 \in X\}, \tag{1}$$

which follows from the following argument

$$\begin{aligned} \frac{\mathbb{E}|Z \cap X|_k}{|Z|_k} &= \frac{\mathbb{E}\int 1\{x \in Z \cap X\}}{|Z|_k} = \frac{\int_Z \mathbb{P}\{x \in X\}dx}{|Z|_k} \\ &= \frac{\int_Z \mathbb{P}\{0 \in X\}dx}{|Z|_k} = \mathbb{P}\{0 \in X\}. \end{aligned}$$

Then by substituting X with $X \oplus rB$ in (1) we get

$$F(r) = \mathbb{P}\{\rho_B(0, X) \leq r\} = \mathbb{P}\{0 \in X \oplus rB\} = \frac{\mathbb{E}\,|Z \cap (X \oplus rB)|_k}{|Z|_k}. \tag{2}$$

Here we should note that the linear first contact distribution (Stoyan et al., 1987) is often defined as

$$H(r) = 1 - \mathbb{P}\{\rho_B(0, X) > r | 0 \notin X\},$$

but we see that F is related to H by

$$H(r) = 1 - \frac{1 - F(r)}{1 - p_X},$$

which means that H easily can be derived from F.

3.1.2. Scale invariance

Let us now consider a scale invariance property of $F(r)$. Above we have chosen a centered structuring element with length 2, and stationarity of the random closed set X implies there is no loss of generality. Indeed, if we assume $B' = (sB)_y,\ s > 0$ and $y \in \mathbb{R}^k$, is a rescaled translated version of

B, then we have

$$\begin{aligned} F_{B'}(r) &= \mathbb{P}\{\rho_{B'}(0,X) \le r\} = \mathbb{P}\{0 \in X \oplus r\check{B}'\} = \mathbb{P}\{0 \in X \oplus r(sB)_y\} \\ &= \mathbb{P}\{0 \in X_{-ry} \oplus (rs)B)\} = \mathbb{P}\{0 \in X \oplus (rs)B\} = F(rs), \end{aligned}$$

hence

$$F(r) = F_{B'}(\frac{r}{s}).$$

3.1.3. Mean star volume

A very interesting feature which has a close connection to the linear contact function is the star volume, which is a measure of the average "local" size of holes in porous materials. Let $X \subset \mathbb{R}^k$ be a stationary random closed set and x_0 a fixed point in $\mathbb{R}^k$. Assume the observation window $W \subset \mathbb{R}^k$ is compact and $|W|_k > 0$, then we define $Y(x_0)$, the star at x_0, by

$$Y(x_0) = \{x \in \mathbb{R}^k : [x_0, x) \subset X^c\}$$

where $[x_0, x)$ denotes the half open line segment with endpoints x_0 and x. Then the mean star volume is defined as

$$v^* = \mathbb{E}\,|Y(x_0)|_k,$$

and is seen by stationarity to be independent of the fixed point x_0. In the isotropic case a simple relation holds between v^* and F. Indeed, letting f denote the density of F, we get by Fubini's theorem, stationarity and change of variable that (Serra, 1982, Chapter X)

$$\begin{aligned} v^* &= \mathbb{E}\int_{\mathbb{R}^k} 1\{[x_0,x) \subset X^c\}dx = \int_{\mathbb{R}^k} \mathbb{P}\{[x_0,x) \subset X^c\}dx = \int_{\mathbb{R}^k} (1 - F(|x_0 - x|/2))dx \\ &= 2\int_{\mathbb{R}^k} (1 - F(|x|))dx = 2\nu_k \int_0^\infty r^{k-1}[1 - F(r)]dr = 2\frac{\nu_k}{k}\int_0^\infty r^k F(dr), \end{aligned}$$

where ν_k is the surface area of the unit ball in $\mathbb{R}^k$. From this we see that v^* does not depend on W and for $k = 3$ we have

$$v^* = \frac{8\pi}{3} \int_0^\infty r^3 F(dr).$$

3.1.4. Chord length distribution

Another interesting feature of the linear contact distribution is that it characterizes the distribution of chord lengths of the complement of X. By using the linear closing of X by B, $X^B = (X \oplus B) \ominus B$ it is possible to define the "length-weighted" distribution G of chord lengths in direction e (i.e. $G(r)$ is the probability that the chord in direction e containing the origin has length $\leq r$), by

$$\begin{aligned} G(r) &= \mathbb{P}\{0 \notin (X^{rB})^c\} \\ &= \frac{\mathbb{E}\,|((X \oplus rB) \ominus rB) \cap W|_k}{|W|_k}. \end{aligned}$$

Further the "unweighted" or "number-weighted" distribution of chord length is

$$G_0(r) = \frac{\int_0^r \frac{1}{t} G(dt)}{\int_0^\infty \frac{1}{t} G(dt)}.$$

Following Matheron (1975, pp. 51-53) we get that F has a density f satisfying

$$G(r) = F(r) - rf(r), \qquad r > 0, \tag{3}$$

and hence

$$G_0(r) = 1 - f(r)/f(0), \qquad r > 0. \tag{4}$$

3.2. Properties of F

To prove properties of F, we need the following construction. Let e be a unit vector in $\mathbb{R}^k$, B defined as in the previous section, and L the line in $\mathbb{R}^k$ with $0 \in L$ and e as directional vector. Choose $e_1, \ldots, e_{k-1}$ such that $\{e_1, \ldots, e_{k-1}, e\}$ is an orthonormal basis of $\mathbb{R}^k$, and define the function

$g : \mathbb{R}^k \to \mathbb{R}^{k-1}$ by $g(x) = (\langle x, e_1\rangle, \ldots, \langle x, e_{k-1}\rangle)$, where $\langle\cdot\rangle$ denotes inner product. Therefore for $y \in \mathbb{R}^{k-1}$, $g^{-1}(y)$ is a line which can be interpreted as a parallel translation of L.

Theorem 1 *Let X be a stationary random closed set in $\mathbb{R}^k$ and W any compact set with $|W|_k > 0$. Then*

1. *The linear contact function F is absolutely continuous and continuously differentiable for $r > 0$ and has an atom at 0 of mass p_X. Moreover, the density f is monotone decreasing.*

2. *The hazard rate of F equals*

$$\lambda(r) = \frac{1}{\mathbb{E}\,|W \setminus (X \oplus rB)|_k} \int_{\mathbb{R}^{k-1}} \mathbb{E}\,\#\{W \cap \partial(g^{-1}(y) \cap (X \oplus rB))\}dy$$

for almost every $r > 0$,

where $\#$ denotes the counting measure and the boundary ∂ is with respect to the Euclidean relative topology on the line $g^{-1}(y)$.

Fig. 3. To get an intuitive idea of the estimator in Theorem 1, see Fig. 3. The proof rests on the following application of geometric measure theory.

Lemma 1 *Let $Z \subset \mathbb{R}^k$ be compact and let $A \subset \mathbb{R}^k$ be any closed set. Then the function $r \mapsto |Z \cap (A \oplus rB)|_k$ is nondecreasing, continuous, and absolutely continuous with*

$$|Z \cap (A \oplus rB)|_k = |Z \cap A|_k + \int_0^r \int_{\mathbb{R}^{k-1}} \#\{Z \cap \partial(g^{-1}(y) \cap (A \oplus sB))\}dy\,ds \tag{5}$$

where ∂ is the boundary w.r.t. the Euclidean relative topology on $g^{-1}(y)$. In particular the integrands are measurable and integrable.

Proof. Two decomposition of measures are used in the proof, first a standard geometric measure decomposition and then Baddeley and Gill (1993, Lemma 1). As the $k-1$ dimensional volume of

the parallelepiped spanned by $e_1, \ldots, e_{k-1}$ is 1, we get that $J_{k-1}\, g(x) = 1$ for all $x \in \mathbb{R}^k$, and by the coarea formula (Federer, 1969, 3.2.22),

$$\begin{aligned} |Z \cap (A \oplus rB)|_k &= \int_Z 1\{x \in A \oplus rB\} dx \\ &= \int_{\mathbb{R}^{k-1}} \int_{g^{-1}(y) \cap Z} 1\{z \in A \oplus rB\} \mathcal{H}^1(dz)\, dy \\ &= \int_{\mathbb{R}^{k-1}} |g^{-1}(y) \cap Z \cap (A \oplus rB)|_1 dy, \end{aligned} \tag{6}$$

where $\mathcal{H}^1$ is the 1-dimensional Hausdorff measure.

With respect to the Euclidean relative topology induced on $g^{-1}(y)$, $g^{-1}(y) \cap A$ is closed. From Baddeley and Gill (1993, Lemma 1) it follows that

$$\begin{aligned} |g^{-1}(y) \cap Z \cap (A \oplus rB)|_1 &= |g^{-1}(y) \cap Z \cap ((g^{-1}(y) \cap A) \oplus rB)|_1 \\ &= |g^{-1}(y) \cap Z \cap A|_1 \\ &\quad + \int_0^r \#\{Z \cap \partial(g^{-1}(y) \cap (A \oplus sB))\} ds. \end{aligned} \tag{7}$$

Insert (7) into (6) and apply Fubini's theorem together with the geometric measure decomposition. □

Proof of Theorem 1. As noted previously the absolute continuity follows from Matheron (1975, pp. 51-53). Moreover from (4) we can conclude that f is monotone decreasing and continuous. The atom at 0 is easily seen by noting that $F(0) = p_X$, so part 1. is proved. Lemma 1 gives (a.s.)

$$|W \cap (X \oplus rB)|_k = |W \cap X|_k + \int_0^r \int_{\mathbb{R}^{k-1}} \#\{W \cap \partial(g^{-1}(y) \cap (X \oplus sB))\} dy\, ds.$$

Since the left side is integrable, Fubini's theorem gives

$$\mathbb{E}\, |W \cap (X \oplus rB)|_k = \mathbb{E}\, |W \cap X|_k + \int_0^r \int_{\mathbb{R}^{k-1}} \mathbb{E}\, \#\{W \cap \partial(g^{-1}(y) \cap (X \oplus sB))\} dy\, ds,$$

whereby 2. follows using equation (2). □

3.3. Random closed sets with $\mathcal{H}^{k-1}$-rectifiable boundary

Recall that a set $A \subset \mathbb{R}^k$ is called $\mathcal{H}^{k-1}$-rectifiable if $\mathcal{H}^{k-1}(A) < \infty$ and there exist Lipschitzian mappings f_j, $j = 1, 2, \ldots$ from some bounded subset of $\mathbb{R}^{k-1}$ onto A_j, $j = 1, 2, \ldots$ and $\mathcal{H}^{k-1}(A \setminus \cup_{j=1}^{\infty} A_j) = 0$. Now restrict attention to $\mathbb{R}^2$ and make the additional assumption on the stationary random closed set X, that $\partial(X \oplus rB)$, is a.s. $\mathcal{H}^1$-rectifiable for all $r \geq 0$, it is possible to show an interesting feature of the hazard rate derived in Theorem 1.

If we rewrite the hazard rate as

$$\lambda(r) = \frac{1}{\mathbb{E}\,|W \setminus (X \oplus rB)|_1} \int_{\mathbb{R}} \mathbb{E}\#\{W \cap g^{-1}(y) \cap \partial(X \oplus rB)\}\, dy,$$

we see that we are counting the number of points of the point process generated by intersecting the fibre process process $\partial(X \oplus rB) \cap W$ with a line $g^{-1}(y)$. This means we can use the theory of fibre processes to derive a somewhat simpler expression for λ, for a review of fibre processes see e.g. Stoyan et al. (1987).

As $\partial(X \oplus rB)$ is assumed to be $\mathcal{H}^1$-rectifiable we know that the angle between e and the fibre tangent at $x \in \partial(X \oplus rB)$ is defined a.s. and will be denoted $w(x)$, which is a number between 0 and π. We can now define the distribution function of the rose of directions for $\partial(X \oplus rB)$ as

$$G_r((0, \alpha]) = \frac{\mathbb{E}\,\mathcal{H}^1(\{x \in \partial(X \oplus rB) \cap W : w(x) \in [0, \alpha]\})}{\mathbb{E}\,\mathcal{H}^1(\partial(X \oplus rB) \cap W)}, \quad \alpha \in (0, \pi],\ r \geq 0.$$

Now restrict the function $g : \mathbb{R}^2 \to \mathbb{R}^1$ defined in Section 3.2 to the set $\partial(X \oplus rB)$ denoted by $g \lfloor \partial(X \oplus rB)$, then simple geometry shows that

$$J_1(g \lfloor \partial(X \oplus rB))(x) = |\sin w(x)|.$$

Using the coarea formula (Federer, 1969, 3.2.22) we get

$$\begin{aligned} & \int_{\partial(X \oplus rB) \cap W} J_1(g \lfloor \partial(X \oplus rB))(x)\ \mathcal{H}^1(dx) \\ = & \int_{\partial(X \oplus rB) \cap W} |\sin w(x)|\ \mathcal{H}^1(dx) \end{aligned}$$

$$= \int_{\mathbb{R}} \int_{g^{-1}(y)} 1\{z \in W \cap \partial(X \oplus rB)\} \, \mathcal{H}^0 dy$$
$$= \int_{\mathbb{R}} \#\{W \cap \partial(X \oplus rB) \cap g^{-1}(y)\} dy.$$

Hence by taking the mean we get the following formula relating the hazard rate of F to the rose of directions of $\partial(X \oplus rB)$

$$\lambda(r) = \frac{\mathbb{E} \int_{\partial(X \oplus rB) \cap W} |\sin w(x)| \, \mathcal{H}^1(dx)}{\mathbb{E} \, |W \setminus (X \oplus rB)|_2}$$
$$= \frac{\mathbb{E} \, \mathcal{H}^1(\partial(X \oplus rB) \cap W)}{\mathbb{E} \, |W \setminus (X \oplus rB)|_2} \int_0^\pi (\sin \alpha) \, G_r(d\alpha).$$

When G_r is the uniform distribution on $(0, \pi]$ as in the case of isotropy (Stoyan et al., 1987, p. 240), then an even simpler formula for λ can be derived

$$\lambda(r) = \frac{2}{\pi} \frac{\mathbb{E} \, \mathcal{H}^1(\partial(X \oplus rB) \cap W)}{\mathbb{E} \, |W \setminus (X \oplus rB)|_2} = \frac{2}{\pi} \frac{\mathbb{E} |\partial(X \oplus rB) \cap W|_1}{\mathbb{E} \, |W \setminus (X \oplus rB)|_2}.$$

For these derivations it is assumed that directions can be parametrised by an angle α in $(0, \pi]$. However, turning to the theory of surface processes the theory extends to $\mathbb{R}^k$, cf. Stoyan et al. (1987).

3.4. The Boolean model

An important example of an analytically tractable model of a random closed set in $\mathbb{R}^k$ is the general stationary Boolean model X. Suppose that Φ_μ is a stationary Poisson point process in $\mathbb{R}^k$ with intensity μ. Let $X_1, X_2, \ldots$ be a sequence of independent identically distributed random closed sets in $\mathbb{R}^k$ that are independent of Φ_μ. Then X is constructed by using "germs" x_n and "grains" X_n

$$X = \cup_{x_n \in \Phi_\mu} (X_n \oplus \{x_n\}).$$

Assume that X_0 is a random closed set and the X_n's are distributed as X_0, then in general it can be shown that, see e.g. Matheron (1975) or Stoyan et al. (1987),

$$F(r) = 1 - \exp\left[-\mu(\mathbb{E} \, |X_0 \oplus rB|_k)\right].$$

Moreover if X_0 is assumed to be a.s. convex and has a distribution which is invariant with respect to rotations about the origin and B is convex then the generalized Steiner formula yields (Stoyan et al., 1987, p. 173)

$$F(r) = 1 - \exp\left[-\frac{\mu}{\omega_k}\sum_{d=1}^{k}\binom{k}{d} r^d \mathbb{E}(W_d(X_0))W_{k-d}(B)\right],$$

where ω_k is the volume of the unit ball in $\mathbb{R}^k$ and W_d denotes the d'th Minkowski functional.

Example 1. If we assume that the X_n's are a.s. spheres with $m_R^{(d)}$ as the d'th moment of the radius distribution then the important planar and spatial cases are as follows for the linear contact function F, and the hazard rate

Planar case (k=2),

$$\begin{aligned} F(r) &= 1 - \exp\left[-2\mu(\pi m_R^{(2)} + 2m_R^{(1)} r)\right] \\ \lambda(r) &= 4\mu m_R^{(1)}. \end{aligned}$$

Spatial case (k=3),

$$\begin{aligned} F(r) &= 1 - \exp\left[-2\pi\mu(\tfrac{2}{3} m_R^{(3)} + m_R^{(2)} r)\right] \\ \lambda(r) &= 2\pi\mu m_R^{(2)}. \end{aligned}$$

Note that the hazard rates are not dependent on r, which can be interpreted as follows. Given one has not met the random set up to distance r then the probability of meeting the set in the next infinitesimal step is constant. This corresponds to the well-known lack of information for Poisson point processes on the real line.

4. Estimation of F

It would be straightforward to construct an estimator of F by means of (2), but it would require information from outside the observation window W, so we make the following construction analogous

to Baddeley and Gill (1993,1994). As in (2) we observe that

$$F(r) = \frac{\mathbb{E}\,|(W \ominus rB) \cap (X \oplus rB)|_k}{|W \ominus rB|_k}. \tag{8}$$

Now define

$$N(r) = |\{x \in W :\ \rho_B(x, X) \leq r,\ \rho_B(x, X) \leq \rho_B(x, \partial W)\}|_k \tag{9}$$

and

$$\begin{aligned} Y(r) &= |\{x \in W :\ \rho_B(x, X) \geq r,\ \rho_B(x, \partial W) \geq r\}|_k \\ &= |(W \ominus rB) \setminus (X \oplus rB)|_k\,, \end{aligned} \tag{10}$$

which are the volume of non-censored points with a distance less than r to the random set and the volume of all points with a distance greater than r to both the random set and the boundary of the window. The quantities can be thought of as the "volume of failures" and "volume at risk", respectively. The two processes are analogous to the number of points counted in the empirical functions $Y(r)$ and $N(r)$ respectively in the definition of the usual Kaplan-Meier estimator, see Andersen et al. (1993). Rewrite $N(r) = |V \cap (X \oplus rB)|_k$ where

$$V = \{x \in W :\ \rho_B(x, X) \leq \rho_B(x, \partial W)\}. \tag{11}$$

Note that $\rho_B(x, \partial W)$ is continuous in x and $\rho_B(x, X)$ is a random upper semi-continuous function and therefore V is measurable for each realization of X. By applying Lemma 1 to each realization we get that $N(r)$ is nondecreasing, continuous, and absolutely continuous on $(0, \infty)$ with density

$$\begin{aligned} \frac{dN(r)}{dr} &= \int_{\mathbb{R}^{k-1}} \#\{V \cap \partial(g^{-1}(y) \cap (X \oplus rB))\}dy \\ &= \int_{\mathbb{R}^{k-1}} \#\{(W \ominus rB) \cap \partial(g^{-1}(y) \cap (X \oplus rB))\}dy. \end{aligned} \tag{12}$$

Hence we get

$$\begin{aligned} \mathbb{E}\,|(W \ominus rB) \cap (X \oplus rB)|_k &= \mathbb{E}|V \cap (X \oplus rB)|_k \\ &= \int_0^r \int_{\mathbb{R}^{k-1}} \mathbb{E}\,\#\{(W \ominus sB) \cap \partial(g^{-1}(y) \cap (X \oplus sB))\}dyds. \end{aligned}$$

The hazard rate for F (see Theorem 1) can also be written using (8) as

$$\lambda(r) = \frac{\int_{\mathbb{R}^{k-1}} \mathbb{E}\,\#\{(W \ominus rB) \cap \partial(g^{-1}(y) \cap (X \oplus rB))\}dy}{\mathbb{E}\,Y(r)}. \tag{13}$$

As F is continuous, with hazard rate $\lambda(r)$ for $r > 0$ and with an atom of mass p_X at 0 we have (Gill, 1994)

$$\begin{aligned} & F(r) \\ = \;& 1 - (1 - p_X) \exp\left(-\int_0^r \lambda(s)ds\right) \\ = \;& 1 - \frac{\mathbb{E}|W \setminus X|_k}{|W|_k} \\ & \times \exp\left(-\int_0^r \frac{1}{\mathbb{E}Y(s)} \int_{\mathbb{R}^{k-1}} \mathbb{E}\#\{(W \ominus sB) \cap \partial(g^{-1}(y) \cap (X \oplus sB))\}dyds\right). \end{aligned} \tag{14}$$

Expressions (8) and (14) then motivate the following definition.

Definition 1 Let X be a stationary random closed set and let $W \subset \mathbb{R}^k$ be a compact set with $|W|_k > 0$. The *Kaplan-Meier estimator* $\widehat{F}^{km}$ of the linear contact function F of X, based on data $X \cap W$ in W, is defined by

$$\begin{aligned} & \widehat{F}^{km}(r) = \\ & \quad 1 - \frac{|W \setminus X|_k}{|W|_k} \exp\left(-\int_0^r \frac{1}{Y(s)} \int_{\mathbb{R}^{k-1}} \#\{(W \ominus sB) \cap \partial(g^{-1}(y) \cap (X \oplus sB))\}dyds\right) \end{aligned} \tag{15}$$

where $Y(r)$ is defined in (10). The *reduced sample estimator* $\widehat{F}^{rs}$ of the linear contact function F of X, based on data $X \cap W$, is defined by

$$\widehat{F}^{rs}(r) = \frac{|(W \ominus rB) \cap (X \oplus rB)|_k}{|W \ominus rB|_k}. \tag{16}$$

Note that (15) and (16) are computable from the data $X \cap W$ and the window W. Analogous to Baddeley and Gill (1993,1994) we have the following properties of $\widehat{F}^{km}$.

Theorem 2 *For an arbitrary closed set X and compact set W with $|W|_k > 0$, the statistic $\widehat{F}^{km}$ is a possibly defective distribution function, i.e. it satisfies the properties of a distribution function but may not necessarily reach 1. Indeed it is continuous and absolutely continuous for $r > 0$, with hazard rate*

$$\widehat{\lambda}(r) = \frac{1}{Y(r)} \int_{\mathbb{R}^{k-1}} \#\{(W \ominus rB) \cap \partial(g^{-1}(y) \cap (X \oplus rB))\} dy$$

and an atom at 0 of mass

$$\widehat{F}^{km}(0) = \frac{|W \cap X|_k}{|W|_k} = \widehat{p}_X = \widehat{F}^{rs}(0).$$

The estimator $\widehat{\lambda}(r)$ of $\lambda(r)$ is ratio unbiased in the sense that

$$\lambda(r) = \frac{\mathbb{E} \int_{\mathbb{R}^{k-1}} \#\{(W \ominus rB) \cap \partial(g^{-1}(y) \cap (X \oplus rB))\} dy}{\mathbb{E}Y(r)}.$$

Proof. The results stated in the theorem are straightforward consequences of Definition 1 and equation (13). □

We saw that $f(r)$ is actually monotone decreasing. Unfortunately $\hat{f}(r) = \hat{\lambda}(r)(1 - \widehat{F}^{km}(r))$ is not necessary monotone, so presumably our estimator could be improved by an isotonization procedure, see e.g. Groeneboom (1985) and Groneboom and Lopuhäa (1993).

5. Implementation

As in Baddeley and Gill (1993,1994) to calculate the estimators described in Definition 1 in practice, one would have to introduce a discretization. If one discretizes the sampling window W on a regular lattice (Serra, 1982), and for each lattice point z_i in W calculates the censored distance from z_i to X, the distance to ∂W and the censoring indicator, i.e. whether or not the distance is censored, then a natural possibility is to calculate the ordinary discrete Kaplan-Meier estimator.

To be more specific, let $\mathbb{Z}_\epsilon = \{\epsilon m : m \in \mathbb{Z}\}$, $\epsilon > 0$. Then $\mathbb{Z}_\epsilon^k = \mathbb{Z}_\epsilon \times \cdots \times \mathbb{Z}_\epsilon$ forms a lattice in $\mathbb{R}^k$ with mesh ϵ.

The next theorem gives sufficient conditions on W and X such that the ordinary discrete Kaplan-Meier and reduced sample estimators converge to the continuous estimators $\widehat{F}^{km}$ and $\widehat{F}^{rs}$, respectively, as the lattice mesh converges to zero.

Theorem 3 *Let X be a random closed set and W a compact set with $|W|_k > 0$. Assume that*

$$|\partial(W \ominus rB)|_k = 0, \qquad r \geq 0, \tag{17}$$

$$|\partial((W \ominus rB) \cap (X \oplus rB))|_k = 0, \qquad \text{a.s. for all } r \geq 0, \tag{18}$$

and

$$|\partial(V \cap (X \oplus rB))|_k = 0, \qquad \text{a.s. for all } r \geq 0, \tag{19}$$

where V is given by (11). For all $z_i \in \mathbb{Z}_\epsilon^k \cap W$, let $t_i = \rho_B(z_i, X \cap W)$, $c_i = \rho_B(z_i, \partial W)$ and $\widetilde{t}_i = \min(t_i, c_i)$, $d_i = 1\{t_i \leq c_i\}$. Construct the discrete Kaplan-Meier estimator

$$\widehat{F}_\epsilon^{km}(r) = 1 - \prod_{s \leq r} \left(1 - \frac{\#\{i : \widetilde{t}_i = s, d_i = 1\}}{\#\{i : \widetilde{t}_i \geq s\}}\right) \tag{20}$$

and the discrete reduced-sample estimator

$$\widehat{F}_\epsilon^{rs}(r) = \frac{\#\{i : t_i \leq r \leq c_i\}}{\#\{i : c_i \geq r\}}. \tag{21}$$

Then as the lattice mesh ϵ converges to zero, $\widehat{F}_\epsilon^{km}(r) \to \widehat{F}^{km}(r)$ and $\widehat{F}_\epsilon^{rs}(r) \to \widehat{F}^{rs}(r)$ for any $r < R$, where

$$R = \inf\{r \geq 0 : (W \ominus rB) \cap (X \oplus rB) = \emptyset\}.$$

Moreover the convergence is uniform on any compact interval in $[0, R)$.

Proof. First let C_ϵ denote the lattice cell centered at the origin, i.e. $C_\epsilon = [-\frac{\epsilon}{2}, \frac{\epsilon}{2}]^k$, $\epsilon > 0$. Then we have for any measurable bounded set $A \subset \mathbb{R}^k$ that

$$A \ominus C_{2\epsilon} \subseteq (\mathbb{Z}_\epsilon^k \cap A) \oplus C_\epsilon \subseteq A \oplus C_{2\epsilon}.$$

By monotonicity of volume

$$|A \ominus C_{2\epsilon}|_k \leq |(\mathbb{Z}^k_\epsilon \cap A) \oplus C_\epsilon|_k \leq |A \oplus C_{2\epsilon}|_k,$$

which leads to

$$|A \ominus C_{2\epsilon}|_k \leq \#(\mathbb{Z}^k_\epsilon \cap A)\epsilon^k \leq |A \oplus C_{2\epsilon}|_k.$$

Now by letting $\epsilon \to 0$, we get

$$|A^\circ|_k \leq \liminf_{\epsilon \to 0} \#(\mathbb{Z}^k_\epsilon \cap A)\epsilon^k \leq \limsup_{\epsilon \to 0} \#(\mathbb{Z}^k_\epsilon \cap A)\epsilon^k \leq |\overline{A}|_k.$$

Furthermore if we assume that $|\partial A|_k = 0$, we have that the limit exists and equals the volume of A, i.e

$$|A|_k = \lim_{\epsilon \to 0} \#(\mathbb{Z}^k_\epsilon \cap A)\epsilon^k.$$

Hence by (17) and (18) the function

$$\begin{aligned} Y_\epsilon(r) &= \#(\mathbb{Z}^k_\epsilon \cap ((W \ominus rB) \setminus (X \oplus rB))) \\ &= \#(\mathbb{Z}^k_\epsilon \cap (W \ominus rB)) - \#(\mathbb{Z}^k_\epsilon \cap ((W \ominus rB) \cap (X \oplus rB))) \end{aligned}$$

converges pointwise to $Y(r)$ as $\epsilon \to 0$. Moreover by (19) the function

$$N_\epsilon(r) = \#(\mathbb{Z}^k_\epsilon \cap (V \cap (X \oplus rB)))$$

converges pointwise to $N(r)$, as $\epsilon \to 0$. Since $N(r)$ is increasing in r and the limit is continuous, $N_\epsilon(r) \to N(r)$ uniformly in r. On the other hand using the fact that $Y(r)$ is decreasing in r with continuous limit we see that $Y_\epsilon(r) \to Y(r)$ uniformly in r. Given (12) and continuity of the mapping $(N, Y) \mapsto 1 - (1 - p_X)\exp(-\int_0^\cdot dN/Y)$, see e.g (Gill, 1994), $\widehat{F}^{km}_\epsilon(r) \to \widehat{F}^{km}(r)$. A similar argument gives the result for $\widehat{F}^{rs}_\epsilon$. □

The following lemma gives sufficient conditions for (17), (18) and (19) to hold for a broad class of random closed sets.

Lemma 2 *Suppose that Φ is a locally finite point process in $\mathbb{R}^k$, i.e. $\Phi(C) < \infty$ a.s. for any bounded Borel set $C \subset \mathbb{R}^k$. Let $X_1, X_2, \ldots$ be a sequence of random closed sets which are a.s. convex sets. Construct the random closed set X by putting*

$$X = \cup_{x_n \in \Phi}(X_n \oplus \{x_n\}). \tag{22}$$

If W is a compact convex set, then X satisfies equations (17), (18) and (19).

Proof. In the following we will use that any convex set $A \subset \mathbb{R}^k$ has $\mathcal{H}^{k-1}$-rectifiable boundary, whereby $|\partial A|_k$=0. As W is assumed convex and rB is convex, we get that $W \ominus rB$ is convex (Matheron, 1975), which immediately gives

$$|\partial(W \ominus rB)|_k = 0, \qquad r \geq 0.$$

Fix a realization of X and notice that

$$(W \ominus rB) \cap (X \oplus rB) = \cup_{x_i \in \Phi}((W \ominus rB) \cap ((X_i)_{x_i} \oplus rB))$$

which is a finite union of convex sets, whence

$$|\partial((W \ominus rB) \cap (X \oplus rB))|_k = 0, \qquad \text{a.s.}$$

We also notice that

$$\begin{aligned} \partial(V \cap (X \oplus rB)) &= \partial(\cup_{x_i \in \Phi} V \cap ((X_i)_{x_i} \oplus rB)) \\ &\subseteq \cup_{x_i \in \Phi} \partial(\{x \in W : \rho_B(x, (X_i)_{x_i}) \leq \rho(x, \partial W)\} \cap ((X_i)_{x_i} \oplus rB)) \\ &= \cup_{x_i \in \Phi} \partial(V_i \cap ((X_i)_{x_i} \oplus rB)), \qquad \text{say.} \end{aligned} \tag{23}$$

Now consider the function $\rho_B(\cdot, \partial W) : W \to \mathbb{R}_+$, and choose $x, y \in W$. Then

$$\begin{aligned} \rho_B(x, \partial W)B + x &\subseteq W \\ \rho_B(y, \partial W)B + y &\subseteq W. \end{aligned}$$

The convex hull of $(\rho_B(x,\partial W)B+x)\cup(\rho_B(y,\partial W)B+y)$ is

$$\begin{aligned} & \mathrm{conv}((\rho_B(x,\partial W)B+x)\cup(\rho_B(y,\partial W)B+y)) \\ = \;& \{\gamma(\rho_B(x,\partial W)b_1+x)+(1-\gamma)(\rho_B(y,\partial W)b_2+y) : b_1,b_2\in B, \gamma\in[0,1]\} \\ \subseteq \;& W, \end{aligned}$$

which implies by choosing $b_1=b_2$, that

$$(\gamma\rho_B(x,\partial W)+(1-\gamma)\rho_B(y,\partial W))B+\gamma x+(1-\gamma)y\subseteq W$$

and thereby

$$\rho_B(\gamma x+(1-\gamma)y,\partial W)\geq\gamma\rho_B(x,\partial W)+(1-\gamma)\rho_B(y,\partial W).$$

We can hereby conclude that $\rho_B(\cdot,\partial W):W\to\mathbb{R}_+$ is a concave function.

On the other hand if we let $K=((X_i)_{x_i}\oplus rB)\cap W$, K is a convex set contained in W. Consider then the function $\rho_B(\cdot,K):W\to\mathbb{R}_+$. Given $x,y\in W$ there exists $b_x,b_y\in B$ such that

$$\begin{aligned} \rho_B(x,K)b_x+x \;&\in\; K \\ \rho_B(y,K)b_y+y \;&\in\; K. \end{aligned}$$

Because K is convex we have that

$$\gamma(\rho_B(x,K)b_x+x)+(1-\gamma)(\rho_B(y,K)b_y+y)\in K,\qquad \gamma\in[0,1],$$

which means that

$$\begin{aligned} & \gamma x+(1-\gamma)y+(\gamma\rho_B(x,K)+(1-\gamma)\rho_B(y,K)) \\ \times \;& \left(\frac{\gamma\rho_B(x,K)}{\gamma\rho_B(x,K)+(1-\gamma)\rho_B(y,K)}b_x+\frac{(1-\gamma)\rho_B(y,K))}{\gamma\rho_B(x,K)+(1-\gamma)\rho_B(y,K)}b_y\right)\in K \end{aligned}$$

i.e.

$$\rho_B(\gamma x+(1-\gamma)y,K)\leq\gamma\rho_B(x,K)+(1-\gamma)\rho_B(y,K).$$

Thus $\rho_B(\cdot, K) : W \to \mathbb{R}_+$ is a convex function.

Because $\rho_B(\cdot, \partial W)$ and $\rho_B(\cdot, K)$ are concave and convex, respectively, $\rho_B(x, K) - \rho_B(x, \partial W)$ is a concave function, hence V_i is a convex set and (23) has volume zero. □

Example 1 continued. If $W \subset \mathbb{R}^k$ is any compact convex window with $|W|_k > 0$, and $X \subset \mathbb{R}^k$ is constructed as in Example 1, the assumptions of Lemma 2 are satisfied.

As noted in Baddeley and Gill (1993,1994) distances $\rho(z, X \cap W)$ and $\rho(z, \partial W)$ (approximations of Euclidean shortest distances) for all points in a fine rectangular lattice can be computed very efficiently using the distance transform algorithm of image processing (Borgefors, 1984; Borgefors, 1986). Similarly if we want to calculate $\rho_B(z, X \cap W)$ and $\rho_B(z, \partial W)$ for horizontal or vertical structuring elements B it is easy to use the forward-backward pass for the one-dimensional case as described in Borgefors (1994), for each horizontal column or vertical row, respectively. If one wants to calculate diagonal distances or even more general line orientations more care is needed. A possibility is to approximate linear behaviour with a highly eccentric Euclidean metric.

6. Analysis of a replicated data set

6.1. Asymptotics

In practical situations, see e.g. Baddeley et al. (1993, Section 2) and Section 6.2 in the present paper, one may, under the assumption of mixing, observe the same random process through a single window which is the union of n small distantly spread windows of fixed size and shape. In this situation the boundary effects stay equally severe as $n \to \infty$, and as in Baddeley and Gill (1993,

Section 4) we shall consider a large sample situation where there are $n \to \infty$ independent replicated observations X_i of a given process X within a fixed window W. Notice in the present paper we do not calculate the pooled statistics $\widehat{F}^{km}$ and $\widehat{F}^{rs}$ as the mean of the separate statistics for each window but by analogies of (15) and (16) where $|W \setminus X|_k$, $\#\{(W \ominus sB) \cap \partial(g^{-1}(y) \cap (X \oplus sB))\}$ and $|(W \ominus rB) \cap (X \oplus rB)|_k$ are replaced by sums of these expressions over all realizations X_i. Asymptotics can now be derived by means of Lemma 3, below. The proof of Lemma 3 uses the result of Giné and Zinn (1984, Theorem 7.4), as in the proof of Baddeley and Gill (1993, Lemma 4). Here we need a slight modification, as explicit bounds on the centered and normed versions of N and Y are difficult to obtain. Moreover this modification removes a convexity assumption on the observation window W.

Lemma 3 *Let $X_1, X_2, \ldots$ be i.i.d. realizations of an a.s. stationary random closed set X. Fix a compact set $W \subset \mathbb{R}^k$ with $|W|_k > 0$ and let $N_i(r)$ and $Y_i(r)$ for $i = 1, 2, \ldots$ be the "fraction of failures" and "fraction at risk" processes corresponding to (9)-(10) for X_i in W, i.e.*

$$N_i(r) = \frac{|\{x \in W : \ \rho_B(x, X_i) \le r, \ \rho_B(x, X) \le \rho_B(x, \partial W)\}|_k}{|W|_k},$$

and

$$Y_i(r) = \frac{|(W \ominus rB) \setminus (X_i \oplus rB)|_k}{|W|_k}.$$

Then

$$n^{1/2} \left(n^{-1} \sum_{i=1}^{n} N_i(r) - \mathbb{E}\frac{N(r)}{|W|_k} \right) \tag{24}$$

and

$$n^{1/2} \left(n^{-1} \sum_{i=1}^{n} Y_i(r) - \mathbb{E}\frac{Y(r)}{|W|_k} \right) \tag{25}$$

converge weakly in $C[0, \tau]$ to Gaussian processes, where $\tau > 0$ satisfies $F(\tau) < 1$, i.e. $\mathbb{E}Y(\tau) > 0$.

Proof. First notice that $N(r)/|W|_k$ and $Y(r)/|W|_k$ are monotone and uniformly bounded by 1. Consider now the normed and centered processes $M = (N - \mathbb{E}N)/|W|_k$ and $Z = (Y - \mathbb{E}Y)/|W|_k$. By Giné and Zinn (1984, Theorem 7.4) the CLT follows if we can show for (24) and (25) separately that

$$\mathbb{E}|M(t) - M(s)| \leq c_1|G(s) - G(t)|$$

and

$$\mathbb{E}|Z(t) - Z(s)| \leq c_2|H(s) - H(t)|$$

for all $s, t \in [0, \tau]$, some constants $c_1, c_2 < \infty$, and some non-decreasing functions G and H. But this is easily seen to be true with $c_1, c_2 = 2$ and

$$\begin{aligned} G(s) &= \frac{\mathbb{E}N(t)}{|W|_k} \\ H(s) &= \frac{\mathbb{E}(Y(0) - Y(s))}{|W|_k}. \end{aligned}$$

□

From Lemma 3 and the marginal tightness of the families (24) and (25) it follows that they are marginally tight and that the finite dimensional distributions satisfy a joint CLT, and therefore a joint CLT for (N, Y) follows. As the product integration mapping is differentiable (Gill and Johansen, 1990, Theorem 8), the functional delta-method (Gill, 1989, Theorem 3) tells us that one can approximate $\widehat{F}^{km} - F$ in probability by the linear expression

$$(1 - F(r)) \times \int_0^r \frac{\int_{\mathbb{R}^{k-1}} \#\{(W \ominus sB) \cap \partial(g^{-1}(y) \cap (X \oplus sB))\}dy - |(W \ominus sB) \setminus (X \oplus sB)|_k \lambda(s)}{(1 - F(s))|W \ominus sB|_k} \, ds. \quad (26)$$

If W is a union of small, distant sub-windows W_i then (26) is also a sum over the W_i of zero-mean terms, given by (26) replacing W by W_i except in the denominator. The variance of $\widehat{F}^{km}(r)$ could

therefore be approximated by the sum of the squares of the summands in (26), in which one would have to replace $\lambda(\cdot)$ and $F(\cdot)$ by their pooled Kaplan-Meier estimates, i.e.

$$\begin{aligned}
&\mathrm{Var}(\widehat{F}^{km}(r) - F(r)) \\
&\doteq \quad (1-\widehat{F}^{km}(r))^2 \sum_{i=1}^{n} \\
&\left[\int_0^r \frac{\int_{\mathbb{R}^{k-1}} \#\{(W_i \ominus sB) \cap \partial(g^{-1}(y) \cap (X \oplus sB))\} dy - |(W_i \ominus sB) \setminus (X \oplus sB)|_k \hat{\lambda}(s)}{(1-\widehat{F}^{km}(s))|W \ominus sB|_k} \, ds \right]^2 .
\end{aligned}$$

6.2. Example data set

Fig. 4. When an image is discretized by a rectangular grid, one can calculate distances by either horizontal or vertical structuring elements as described in Section 5. In the present example we calculated the pooled Kaplan-Meier estimator in both directions, see equation (27) below, for all experimental groups. In Fig. 4 we plot $-\log(1-\widehat{F}^{km}(r))$ against r, the estimator is shown surrounded by its 95% pointwise confidence interval, see later. For (a)-(c) there seems to be a slight tendency to anisotropy and for (d) the plot does not give any reason to doubt isotropy. However to develop the methodology we chose to pool the estimator over both directions to see if we could get a decrease in variance. Fig. 5 shows the ratio of the estimated variances of the Kaplan-Meier estimator in horizontal and vertical directions to the estimated variance of the pooled estimator. For the vertical direction there is a clear gain in pooling over directions, whereas for the horizontal estimator the gain is only achieved in case (a)-(c) for small distances. This also gives some evidence for anisotropy which should be investigated further.

Fig. 5. If isotropy is assumed, pooling the estimator over directions can be justified by the following. Let $\widetilde{B}$ be the structuring element B rotated through 90°, and consider the following modified estimators from Definition 1.

$$\widehat{F}^{km}(r) = 1 - \frac{|W \setminus X|_k}{|W|_k} \exp\left(- \int_0^r \frac{dN(s) + d\widetilde{N}(s)}{Y(s) + \widetilde{Y}(s)} ds \right) \tag{27}$$

$$\widehat{F}^{rs}(r) = \frac{|(W \ominus rB) \cap (X \oplus rB)|_k + |(W \ominus r\widetilde{B}) \cap (X \oplus r\widetilde{B})|_k}{|W \ominus rB|_k + |W \ominus r\widetilde{B}|_k},$$

where N and Y are calculated w.r.t. B and $\widetilde{N}$ and $\widetilde{Y}$ w.r.t. $\widetilde{B}$. It is straightforward to see that the new estimator $\widehat{F}^{rs}$ is unbiased, but also the results from Theorem 2 are carried over to the new estimator $\widehat{F}^{km}$. Of practical importance is that the implementation as suggested in Theorem 3 also works for the pooled estimator. With superscript h denoting measurements along the horizontal direction and v denoting measurements along the vertical direction we get the following pooled versions of (20) and (21).

$$\widehat{F}^{km}_{\epsilon}(r) = 1 - \prod_{s \le r} \left(1 - \frac{\#\{i : \widetilde{t}_i^h = s, d_i^h = 1\} + \#\{i : \widetilde{t}_i^v = s, d_i^v = 1\}}{\#\{i : \widetilde{t}_i^h \ge s\} + \#\{i : \widetilde{t}_i^v \ge s\}} \right)$$

$$\widehat{F}^{rs}_{\epsilon}(r) = \frac{\#\{i : t_i^h \le r \le c_i^h\} + \#\{i : t_i^v \le r \le c_i^v\}}{\#\{i : c_i^h \ge r\} + \#\{i : c_i^v \ge r\}}.$$

Fig. 6. For the replicated image data set described in Section 2 and illustrated in Fig. 1, the implementation described in Section 5 and above was applied. The pooled Kaplan-Meier and reduced sample estimators were calculated as described in Section 6.1 and are plotted in Fig. 6. For each experimental group we see the estimator in the middle surrounded by its 95% pointwise confidence interval. The variance of the Kaplan-Meier estimator is calculated by means of the discretized version of the influence function given by (26). By invoking the CLT, the pointwise 95% confidence intervals are based on the normal distribution. For the reduced sample estimator, we just calculated the ordinary pointwise 95% confidence intervals for the normal distribution by the sample standard deviation of the 12 replicates as the overall reduced sample estimator is simply the pointwise mean of the independent individual estimators. We observe that the discrepancies between the Kaplan-Meier

and reduced sample estimators are very slight. This corresponds to other results for real data sets reported in Baddeley and Gill (1994). However, it is possible to produce artificial data for which the Kaplan-Meier and reduced sample estimators differ appreciably.

Fig. 7. In Fig. 7 (a) and (b) we observe that the estimated curve for short exposure and its pointwise 95% confidence intervals lie all above the same curves for long exposure, giving strong evidence for difference between heat treatments at the two magnifications, moreover from (c) and (d) there is an overlap of the confidence intervals giving no reason to believe an effect of magnification.

Fig. 8. Fig. 8 shows the empirical relative efficiencies (ratio of the variances of reduced sample to Kaplan-Meier estimator calculated in connection with Fig. 6), for each experimental group. The general pattern is that the greatest gain is achieved at small distances except for (b), and for larger distances the gain in efficiency is decreasing, again except for (b) where there seems to be a gain of efficiency. The results from (a), (c) and (d) correspond to the patterns found in Baddeley and Gill (1993). From this it seems that the bias of the Kaplan-Meier estimator (because the reduced sample estimator is unbiased) is of smaller order than the variance, so the estimators agree well, but have different variance.

Table 1. As the variance of the Kaplan-Meier estimator is smaller than the variance of the reduced sample estimator and the bias generally seems to be of smaller order than the variance, we have fitted a 3-dimensional Boolean model of spheres with fixed radii R to the Kaplan-Meier estimator, see Example 1. Using a nonlinear least squares procedure (the `nls` function in S-PLUS) fitting the function $1 - \exp(-2\pi\mu((2/3)R^3 + R^2 r))$ to the pooled estimators $\widehat{F}^{km}(r)$ in each experimental group, we obtained the estimates shown in Table 1. The standard error of the estimates in Table 1 is derived by the following simple jackknife procedure (Efron and Tibshirani, 1993, Chapter 11). Suppose we have the sample $((N_1, Y_1), \ldots, (N_{12}, Y_{12}))$ of "fraction of failures" and "fraction at risk"

processes and the estimator

$$\hat{\theta}((N_1, Y_1), \ldots, (N_{12}, Y_{12})) = (\hat{\theta}^1, \hat{\theta}^2) = (\hat{\mu}, \widehat{R})$$

where

$$\begin{aligned} & \int_0^\infty \left[(1 - \exp(-2\pi\hat{\mu}((2/3)\widehat{R}^3 + \widehat{R}^2 r))) - \widehat{F}^{km}(r)\right]^2 dr \\ = & \min_{(\mu,R)\in\mathbb{R}_+^2} \int_0^\infty \left[(1 - \exp\{-2\pi\mu[(2/3)R^3 + R^2 r]\}) - \widehat{F}^{km}(r)\right]^2 dr \end{aligned}$$

and $\widehat{F}^{km}$ is the pooled estimator based on all 12 replications. Then the jackknife estimate of standard error of the k'th coordinate, $k = 1, 2$, is defined by

$$\hat{s}_k = \left[\frac{n-1}{n}\sum_{i=1}^{n}(\hat{\theta}^k_{(i)} - \hat{\theta}^k_{(\cdot)})^2\right]^{1/2}, \qquad k = 1, 2$$

where $\hat{\theta}_{(i)} = (\hat{\theta}^1_{(i)}, \hat{\theta}^2_{(i)})$ is the i'th jackknife sample which consists of the data set with the i'th observation removed and

$$\hat{\theta}_{(\cdot)} = \sum_{i=1}^{n} \hat{\theta}_{(i)}/n.$$

Fig. 9. To check whether the distribution function is fitted appropriately, we use the transformation,

$$\arcsin(\sqrt{1 - F(t)}),$$

which is known to stabilize the variance asymptotically for estimations of F based on i.i.d. observations of the distribution function F (Aitkin and Clayton, 1980). In Fig. 9 the transformation $\arcsin((1 - \widehat{F}^{km}(r))^{\frac{1}{2}})$ of the Kaplan-Meier estimator is plotted against the transformation of the fitted distribution function. We see that there is a possible misspecification at the first point for all experimental groups. For all groups we also notice that there is a slight deviation for large distances. Moreover, for (a) we have some discrepancy for small distances. But in general this plot does not reject the Boolean model over a large interval of intermediate values.

Returning to the fit in Table 1, the radius around 0.5-0.6 μm seems to be too large (the mean particle diameter in suspension before heat treatment is believed to be around 0.15 μm). However,

several explanations can be given for that. Firstly, it is hypothesised that the protein particles clump together under heat treatment and therefore form larger clumps and secondly it is believed that the network created under the subsequent fermentation process is a diffusion limited process, so no overlap between particles is possible, which is the case in the Boolean model. From the estimates we also notice that the clumps get larger under further heat treatment, additionally support for the hypothesis that heat treatment creates larger and larger clumps.

Visually, see Fig. 1, heat treatment seems to have the same effect as magnification from $\times 5000$ to $\times 7500$. As the volume content, $\hat{p}_X$, is almost the same in all experimental groups and a Boolean model has been fitted, we calculated the ratios between the hazard rates for short and long treatment, obtaining the values 1.42 and 1.47 for $\times 5000$ $\times 7500$ respectively. The values close to 1.5 support the visual impression, and also support the idea that particles become larger under heat treatment, but have the same shape and that the network under different heat treatments is created under the same diffusion regime.

From Section 3.1.3 we know that the star volume can be expressed by the linear contact function; a simple "plug-in" estimate of the star volume is therefore

$$\hat{v}^* = \frac{8\pi}{3} \int r^3 \widehat{F}^{km}(dr).$$

Table 2. These estimates for each experimental group can be seen in Table 2. The standard error of the star volume given in Table 2 is derived analogously to Table 1 by means of jack-knifing. Here the estimator $\hat{\theta}$ is simply

$$\hat{\theta}((N_1, Y_1), \ldots, (N_{12}, Y_{12})) = \frac{8\pi}{3} \int r^3 \widehat{F}^{km}(dr).$$

Here we observe a statistically significant effect of heat treatment, the star becomes bigger as the particles clump more together. Moreover, there is a little evidence of a magnification effect. This could be explained by the fact that more details appear at a higher magnification rate.

Fig. 10. Fig. 10 shows an estimate of the first contact hazard function $\lambda(r)$ in each experimental group. The solid line shows the pointwise estimate obtained by the discrete hazard function, pooled over both images and directions

$$\hat{\lambda}(r) = \frac{\#\{i : \tilde{t}_i^h = r, d_i^h = 1\} + \#\{i : \tilde{t}_i^v = r, d_i^v = 1\}}{\#\{i : \tilde{t}_i^h \geq r\} + \#\{i : \tilde{t}_i^v \geq r\}}. \tag{28}$$

To apply kernel smoothing to the hazard rate, see the dotted line in Fig. 10, we have to take into account the substantial increase in variance over the range of distances as we approach the endpoints of support for the empirical hazard rate. Here we consider the variable kernel method (Silverman, 1986, Section 2) to smooth the Nelson estimator given in (28), with the Parzen kernel and a variable bandwidth increasing from 0.37 μm to 1.05 μm for $\times$7500 magnification, and from 0.25 μm to 1.0 μm for $\times$5000 magnification. This seems somewhat arbitrary but by inspection the smoothing seems to give reasonable results. It should however be noted that quite sophisticated techniques exist for smoothing hazard rates under random censoring (Müller and Wang, 1994), but as we are mainly interested in the deviance from the fitted boolean model it does not seem to be of any help to apply these techniques.

It is clear that there is a difference of the course of the hazard rate under different heat treatments, both in the level and shape of the hazard curve. According to Section 3.4 we would expect the hazard rate to be a horizontal line if the data were generated by a Boolean model. This seems reasonable for intermediate distances in case (b) and (d), but for (a) and (c) there seems to be a general drop in the hazard rate. Furthermore in all situations (a)-(d) there seems to be a slight drop from the start. Problems with the Boolean model in the start were also noticed in Fig. 9. A close look at Fig. 9 (a) and (c) also suggest a slight misspecification for intermediate distances. The drop at the start could be a consequence of the network structure as one might expect that the particles are more clustered. Another explanation could be that the erosion in the image cleaning process has deleted small clumps. So finally we must conclude that the Boolean model for short exposure is not a good

fit to the data, but seems to be a reasonable model for the long heat treatment.

7. Discussion

In this paper we have shown continuity, absolute continuity and continuous differentiability of the linear contact distribution function F, for any stationary random closed set X. Moreover, we developed a Kaplan-Meier type estimator for F, demonstrated, and compared it with the reduced sample estimator on a replicated data set, and concluded that the Kaplan-Meier estimator in this example is more efficient than the reduced sample estimator, and the bias is of smaller order than the variance.

Replication has been used to calculate standard errors for the pooled estimates. This is a new approach, (recently introduced in (Baddeley et al., 1993), although with another approach for the variance calculation), since it is normal in spatial statistics to produce pointwise confidence intervals around the theoretical Boolean curve rather than confidence intervals around the empirical curve. We also suggested when estimating the linear contact function under isotropy to pool the estimator over directions to decrease variance.

Our conclusions about the data set are that

1. some evidence for anisotropy has been spotted;
2. there is a significant difference in the linear contact function over different heat treatments;
3. a Boolean model seems reasonable for long exposure, but does not fit well for the short heat treatment;
4. there is some evidence for clustering of the particles;
5. heat treatment seems to increase the particle size, and as the protein content stays the same, the density of particles per unit volume decreases;

6. heat treatment seems to have the same effect as magnification, supporting the hypothesis that under heat treatment the particles clump together, and the subsequent coagulation process is the same.

In this application all the windows had the same size and shape, but the number n of replications was small, so one could argue that the formal asymptotics as done for the data set cannot give a very accurate picture. Therefore simulation experimentation is needed to compare the worth of the various standard error estimates in practical situations.

It should be noted that another competing estimator has been developed recently by Chiu and Stoyan (1994). This estimator, denoted the Hanisch estimator, has been developed for stationary random closed sets and a general structuring element. The estimator is unbiased, but has the disadvantage that it can exceed 1. This can be dealt with by different kinds of normalizations, but then the advantage of unbiasedness disappears. This estimator could be applied to the data, but would require a substantial development and is therefore beyond the scope of the present paper.

The discussion about edge correction could also be continued by considerations about the importance of sampling points. This problem arises as there seem to be more of an edge problem for points near the boundary than say points well inside the observation window. An attempt to deal with that could be to implement Anbeek's (1993) suggestion for a weighted Kaplan-Meier estimator in the case of interpoint distributions for spatial point processes. Here it is suggested to give less weight to the sampling points close to the border of the window.

It was noted in Section 3.1.1 that a 1-1 relationship holds between the two distribution functions H and F. This means that all the regularity properties of F derived in the paper can be carried over to H. A consequence of this is that H and F has the same hazard rate and H is therefore estimated by the relation

$$\widehat{H}(r) = 1 - \frac{1 - \widehat{F}(r)}{1 - \hat{p}_X}.$$

From a distributional point of view it does not matter where the structure element is centered and how long it is, see Section 3.1.2, but from the viewpoint of estimation it could make a difference, especially the centering is sensitive to the behaviour at the boundary.

For cross-sectional images such as those displayed in Fig. 1, we saw that the linear structuring element could be used to draw inferences about the star volume and the 3-dimensional Boolean model. It should also be noted that other elements with empty interior could be considered, such as disks or squares as they do not require information from the missing dimension. A collection of such elements could then be used to derive more robust estimators for random set models along the lines reviewed e.g. in Cressie (1991, Section 9.5).

The idea of using the hazard rate of the empty space function F for a spatial pattern has appeared in various guises in the literature; Miles (1970,1974) show that many distance variables in stochastic geometry are closely connected to one-dimensional waiting times. Furthermore, Daley and Vere-Jones (1988, pp. 242-245) discuss the survival function and hazard rate of the empty space function for Poisson processes. Baddeley and Gill (1994) present calculations of the hazard rate for some well known data sets. However the estimation in Fig. 10, shows that all the classical problems of density estimation are present in the data set (Silverman, 1986) such as discretization problems, bandwidth selection, bias variance trade-off and kernel choice. New problems also arise here, e.g. digitization problems (Serra, 1982) and image cleaning problems, so therefore one should be cautious about interpreting the hazard rates in Fig. 10, until the method is better understood.

Despite the fact that the Boolean model gave some interesting information about the process, it should only be considered as a preliminary model, as the network is formed under diffusion and not by for instance continuum percolation. Another interesting alternative would be to model the underlying point process by the recently suggested area-interaction point processes (Baddeley and van Lieshout, 1995), as they produce a great variety of clustered behaviour. This is of course closer

to reality but still seems away from the diffusion regime.

The conclusions found in points 1-6 above could be investigated further for instance using other structuring elements, or by investigation of the distribution of single particles under random censoring, see e.g. Molchanov (1992,1994), but this is outside the scope of this paper and will be reported elsewhere (Hansen, 1995). Another approach to analyse the network, which has not been pursued here, is to plug in an estimator for the linear contact distribution in the expression (3), e.g. the Kaplan-Meier or another edge corrected estimator, to provide an edge corrected estimate of either the weighted or unweighted chord length distribution.

Computational and software aspects of our approach will be presented elsewhere.

Acknowledgments

We thank Anne Skriver for supplying the data set and Murray Aitkin and Ilya Molchanov for helpful comments. Martin B. Hansen would like to thank Dina, (Danish Informatics Network in the Agricultural Sciences) and Føtek, (Centre for Food Research, RVAU) for financial support and The Danish Research Academy for the grant which made it possible to visit University of Utrecht during the spring semester 1994. Adrian Baddeley's research was partially funded by CWI, Amsterdam and NWO (Netherlands Scientific Research Organisation). The useful comments of the referees and the editor are also acknowledged.

References

Aitkin, M. and Clayton, D. (1980). The fitting of exponential, Weibull and extreme value distributions to complex censored survival data using GLIM. *Applied Statistics*, 29:156–163.

Anbeek, N. (1993). The Weighted Kaplan-Meier Estimator. Master's thesis, University of Utrecht, Department of Mathematics.

Andersen, P. K., Borgan, Ø., Gill, R. D., and Keiding, N. (1993). *Statistical Models Based on Counting Processes.* Springer, New York.

Baddeley, A. J. and Gill, R. D. (1993). Kaplan-Meier estimators of interpoint distance distributions for spatial point processes. Research Report BS-R9315, Centrum voor Wiskunde en Informatica. Submitted for Publication.

Baddeley, A. J. and Gill, R. D. (1994). The empty space hazard of a spatial pattern. Research Report Feb. 1994/3, Department of Mathematics, The University of Western Australia. Submitted for Publication.

Baddeley, A. J., Moyeed, R. A., Howard, C. V., and Boyde, A. (1993). Analysis of a three-dimensional point pattern with replication. *Applied Statistics*, 42:641–668.

Baddeley, A. J. and van Lieshout, M. N. M. (1995). Area-interaction point processes. To appear in *Annals of the Institute of Statistical Mathematics.*

Borgefors, G. (1984). Distance transformations in arbitrary dimensions. *Computer Vision, Graphics and Image Processing*, 27:321–345.

Borgefors, G. (1986). Distance transformations in digital images. *Computer Vision, Graphics and Image Processing*, 34:344–371.

Chiu, S. N. and Stoyan, D. (1994). Estimators of distance distributions for spatial patterns. Manuscript submitted for publication.

Cressie, N. A. C. (1991). *Statistics for Spatial Data.* John Wiley and Sons, New York.

Daley, D. J. and Vere-Jones, D. (1988). *An introduction to the theory of point processes.* Springer, New York.

Efron, B. and Tibshirani, R. (1993). *An Introduction to the Bootstrap*, volume 57 of *Monographs on Statistics and Applied Probability.* Chapman and Hall, London.

Federer, H. (1969). *Geometric Measure Theory.* Springer Verlag, Heidelberg.

Gill, R. D. (1989). Non- and semiparametric maximum likelihood estimators and the von Mises method, I. *Scand. J. Statist.*, 16:97–128.

Gill, R. D. (1994). Lectures on survival analysis. In Bernard, P., editor, *Lectures on Probability Theory, Ecole d'Eté de Probabilités de Saint-Flour XXII 1992.* Lecture Notes in Mathematics. Springer.

Gill, R. D. and Johansen, S. (1990). A survey of product-integration with a view toward application in survival analysis. *Ann. Stat.*, 18:1501–1555.

Giné, E. and Zinn, J. (1984). Some limit theorems for empirical processes. *Annals of Probability*, 12:929–989.

Groeneboom, P. (1985). Estimating a monotone density. In Cam, L. L. and Olshen, R., editors, *Proceedings of the Berkeley conference in Honor of Jerzy Neyman and Jack Kiefer, Vol. II*, pages 539–555, Monterey. Wadsworth.

Groeneboom, P. and Lopuhäa, H. (1993). Isotonic estimators of monotone densities and distribution functions. *Statistica Neerlandica*, 47:175–184.

Hall, P. (1988). *Introduction to the Theory of Coverage Processes.* John Wiley and Sons, New York.

Hansen, M. B. (1995). *Spatial Statistics for Network Structures in Processed Milk.* PhD thesis, Dina Research Report no. 30.

Kaplan, E. and Meier, P. (1958). Nonparametric estimation from incomplete observations. *J. Amer. Statist. Assoc.*, 53:457–481.

Kolmogorov, A. and Leontovitch, M. (1992). On computing the mean Brownian area. In Shiryaev, A., editor, *Selected works of A.N. Kolmogorov, Volume II: Probability and mathematical statistics*, volume 26 of *Mathematics and its applications (Soviet series)*, pages 128–138. Kluwer, Dordrecht–Boston–London.

Laslett, G. M. (1982). The survival curve under monotone density constraints with applications to two-dimensional line segment processes. *Biometrics*, 69:153–160.

Matheron, G. (1975). *Random Sets and Integral Geometry.* John Wiley and Sons, New York.

Miles, R. G. (1970). On the homogeneous planar Poisson point process. *Mathematical Biosciences*, 6:85–127.

Miles, R. G. (1974). On the elimination of edge-effects in planar sampling. In Harding, E. F. and Kendall, D. G., editors, *Stochastic geometry: a tribute to the memory of Rollo Davidson*, pages 228–247, London, New York, Sydney, Toronto. John Wiley and Sons.

Molchanov, I. S. (1992). Handling with spatial censored observations in statistics of Boolean models of random sets. *Biom. J.*, 34:617–631.

Molchanov, I. S. (1994). On statistical analysis of Boolean models with non-random grains. *Scand. J. Statist.*, 21:73–82.

Müller, H. G. and Wang, J. L. (1994). Hazard rate estimation under random censoring with varying kernels and bandwidths. *Biometrics*, 50:61–76.

Robbins, H. (1944). On the measure of a random set. *Annals of Mathematical Statistics*, 15:70–74.

Robbins, H. (1945). On the measure of a random set II. *Annals of Mathematical Statistics*, 16:342–347.

Robbins, H. (1947). Acknowledgement of priority. *Annals of Mathematical Statistics*, 18:297.

Serra, J. (1982). *Image Analysis and Mathematical Morphology.* Academic Press.

Silverman, B. W. (1986). *Density Estimation for Statistics and Data Analysis.* Chapman and Hall, London.

Skriver, A., Hansen, M. B., and Qvist, K. B. (1995). Image analysis applied to electron micrographs of stirred yoghurt. Preprint, Royal Veterinary and Agricultural University, Copenhagen. Submitted for publication.

Stoyan, D., Kendall, W. S., and Mecke, J. (1987). *Stochastic Geometry and Its Applications.* John Wiley and Sons and Akademie Verlag, Chichester and Berlin.

Martin B. Hansen, Aalborg University, Institute for Electronic Systems, Department of Mathematics and Computer Science, Frederik Bajersvej 7E, DK-9220 Aalborg Ø, Denmark.

Richard Gill, Mathematical Institute, University of Utrecht, Budapestlaan 6, 3584 CD Utrecht, The Netherlands.

Adrian Baddeley, Department of Mathematics, University of Western Australia, Nedlands WA 6009, Australia.

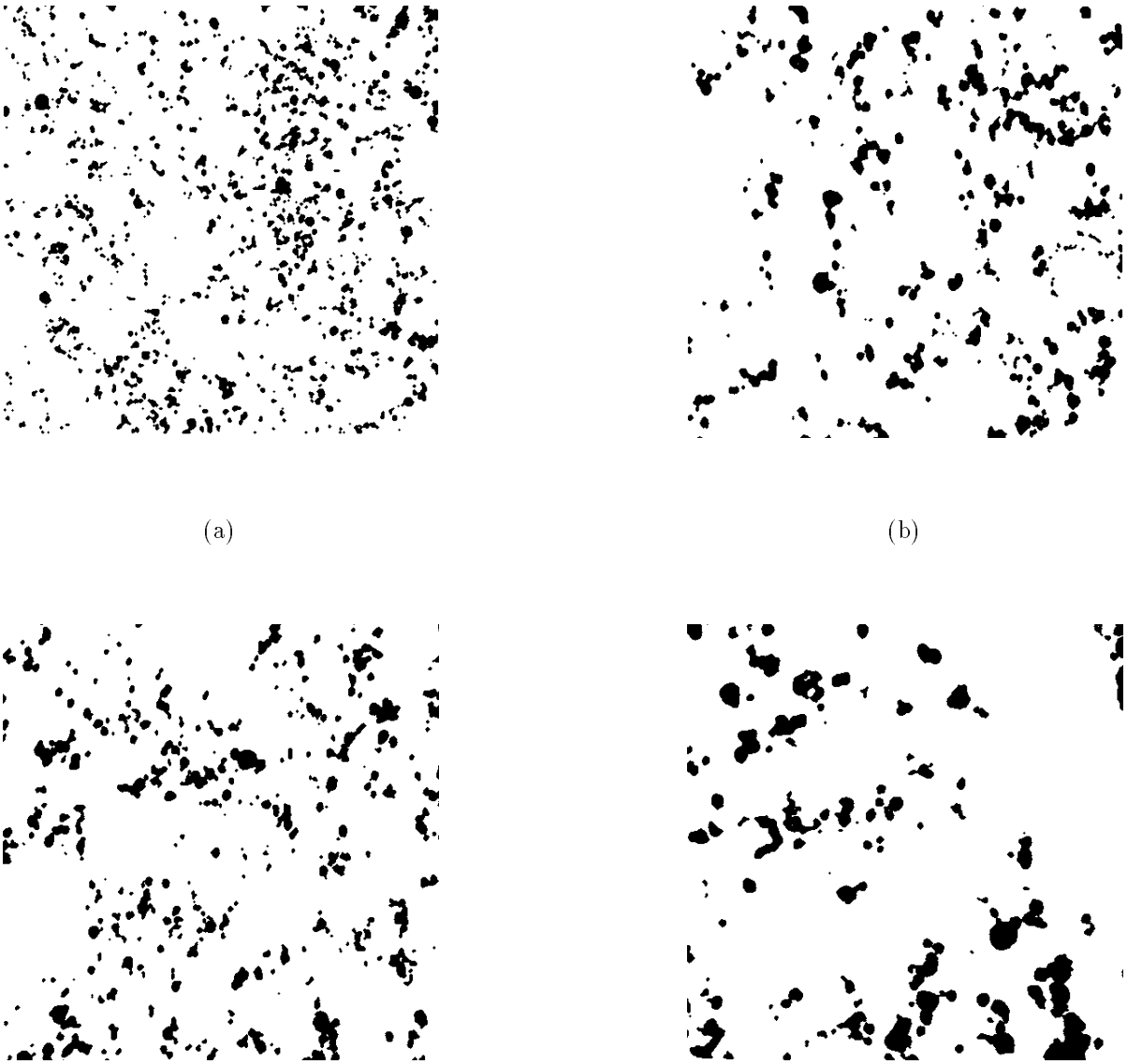

(a) (b)

(c) (d)

Fig. 1. Protein network (represented by black) in a yoghurt ferment. (a) ×5000, short; (b) ×5000, long; (c) ×7500, short; (d) ×7500, long. For magnification ×5000, the physical scale of the image is a square with side length 37.10 μm, and for ×7500, sidelength 24.73 μm.

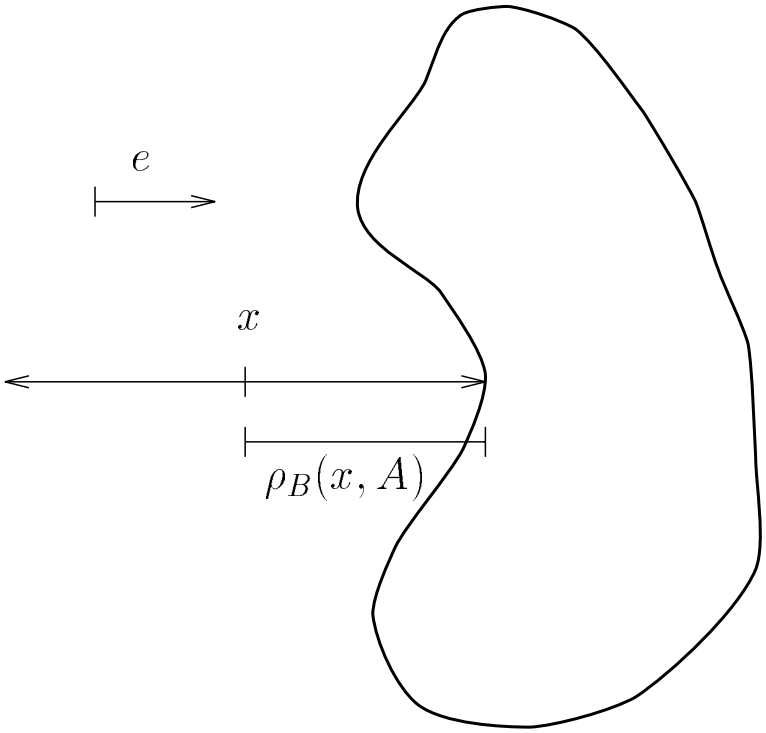

Fig. 2. In the text we have defined $\rho_B(x, A)$ to be the "shortest" distance to A from x "looking in both ways" along the directional vector e.

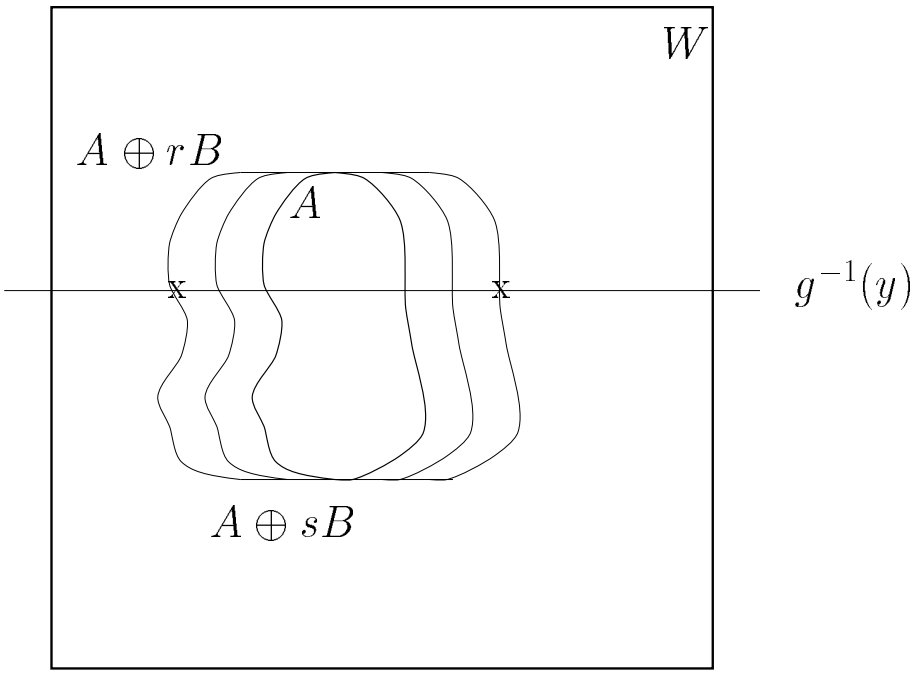

Fig. 3. The x's mark the points of the set $\#\{W \cap \partial(g^{-1}(y) \cap (A \oplus rB))\}$, which is used throughout the paper.

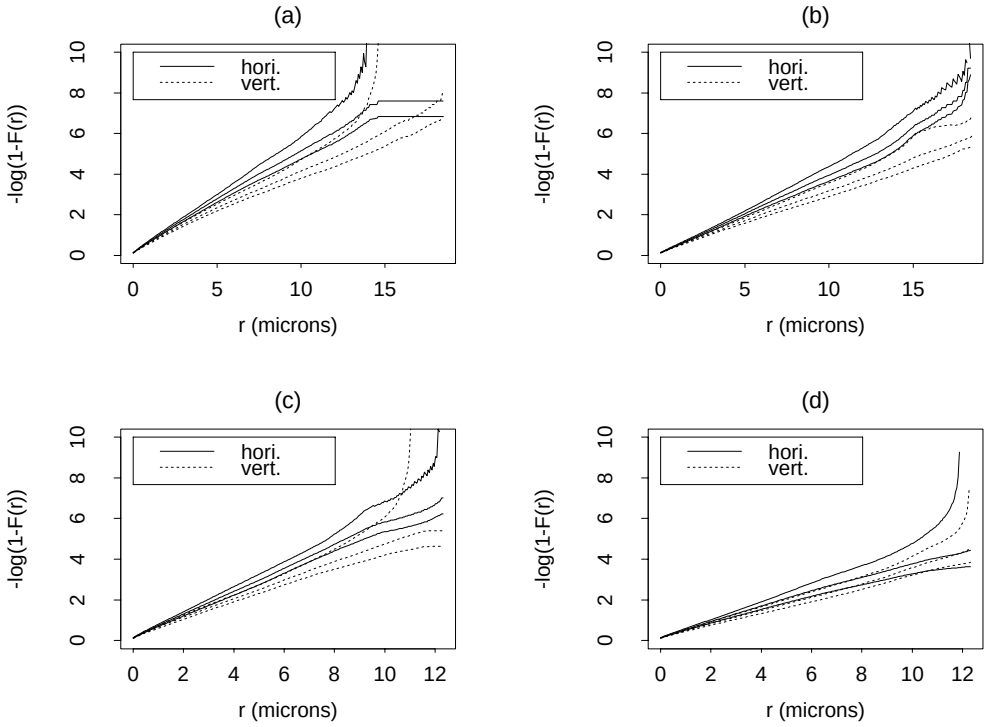

Fig. 4. Plot of $-\log(1-\widehat{F}^{km}(r))$ against r, for the pooled Kaplan-Meier estimator in horizontal and vertical directions. (a) $\times 5000$, short; (b) $\times 5000$, long; (c) $\times 7500$, short; (d) $\times 7500$, long.

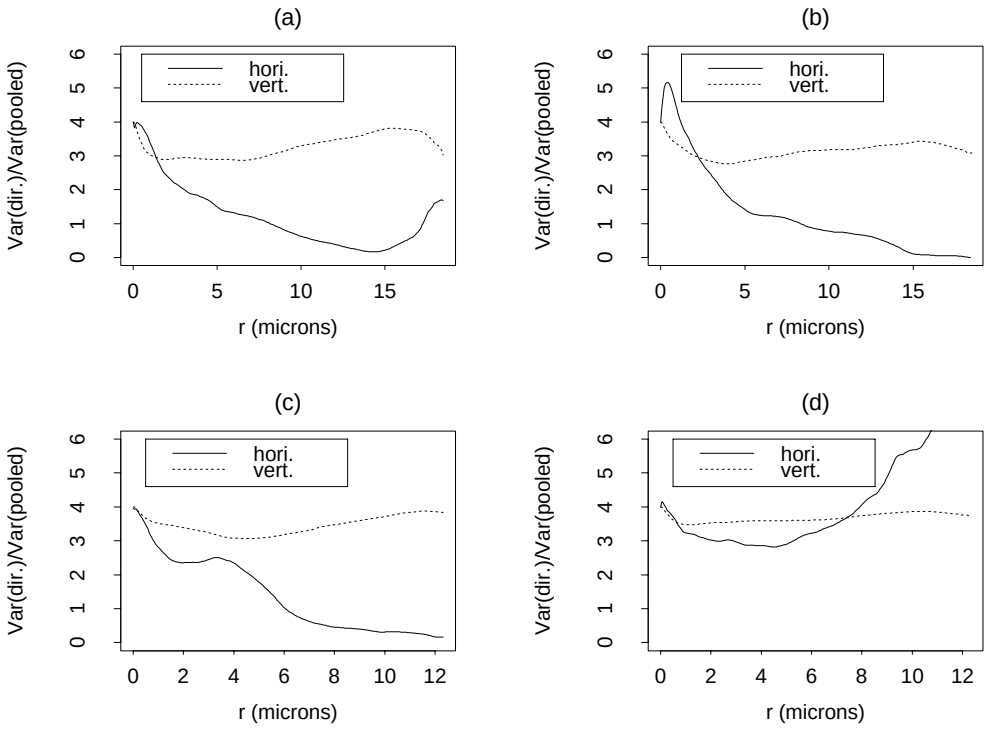

Fig. 5. Ratio of the estimated variance of the Kaplan-Meier estimator in horizontal and vertical directions to the estimated variance of the pooled estimator. (a) $\times 5000$, short; (b) $\times 5000$, long; (c) $\times 7500$, short; (d) $\times 7500$, long.

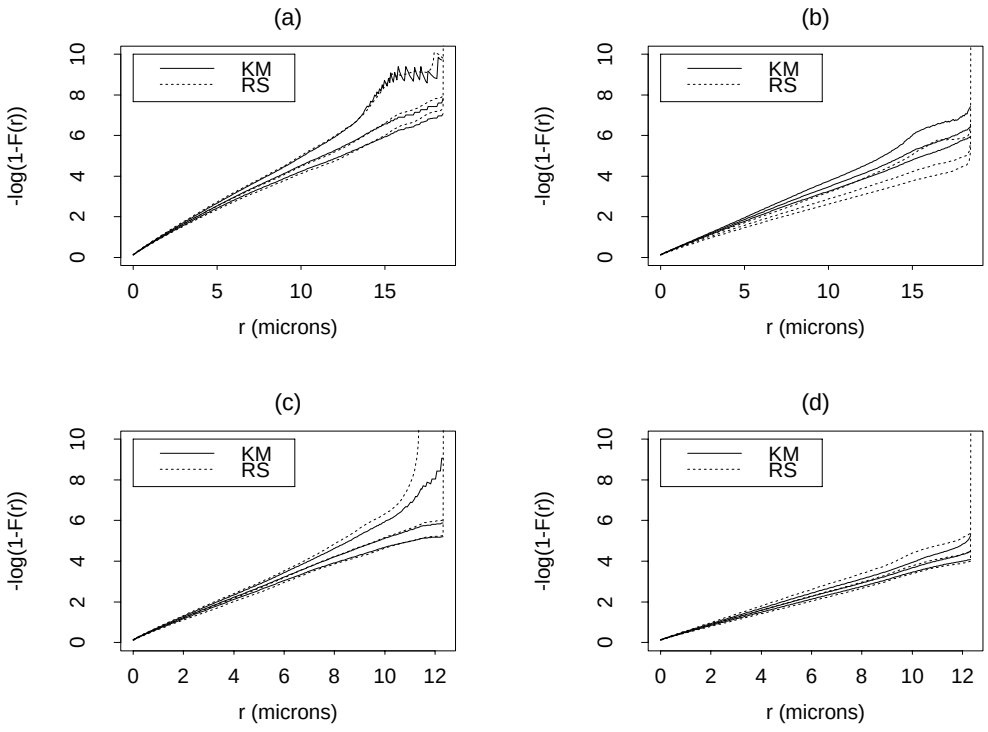

Fig. 6. Plot of $-\log(1-\widehat{F}(r))$ against r, for the pooled Kaplan-Meier and reduced sample estimators of the linear contact function in each experimental group. (a) $\times$5000, short; (b) $\times$5000, long; (c) $\times$7500, short; (d) $\times$7500, long.

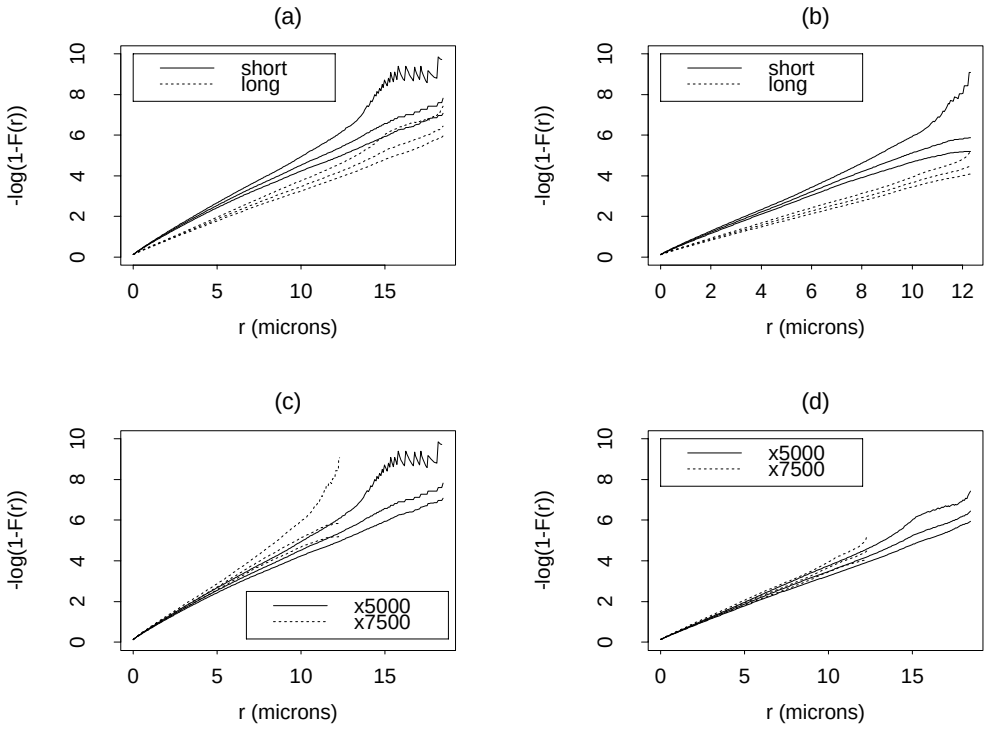

Fig. 7. Plot of $-\log(1-\widehat{F}^{km}(r))$ against r, for the pooled Kaplan-Meier estimator. (a) The estimators for short and long heat treatment for magnification $\times 5000$; (b) The estimators for short and long heat treatment for magnification $\times 7500$; (c) The estimators for $\times 5000$ and $\times 7500$ for short heat treatment; (d) The estimators for $\times 5000$ and $\times 7500$ for long heat treatment.

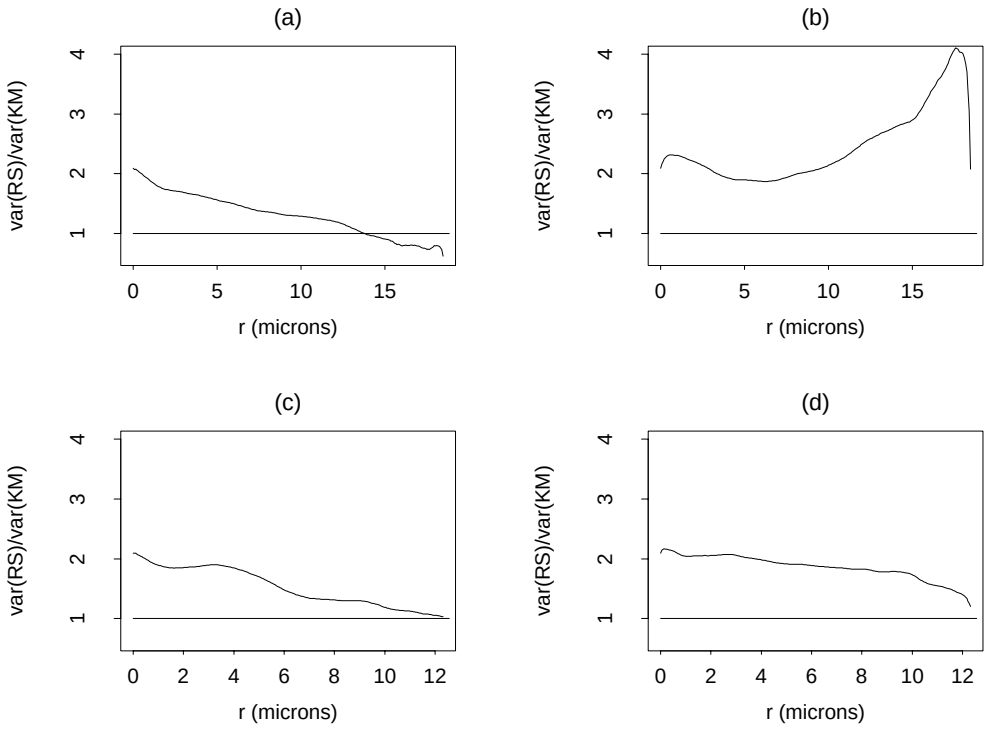

Fig. 8. The relative efficiency of KM over RS in each experimental group. (a) $\times 5000$, short; (b) $\times 5000$, long; (c) $\times 7500$, short; (d) $\times 7500$, long.

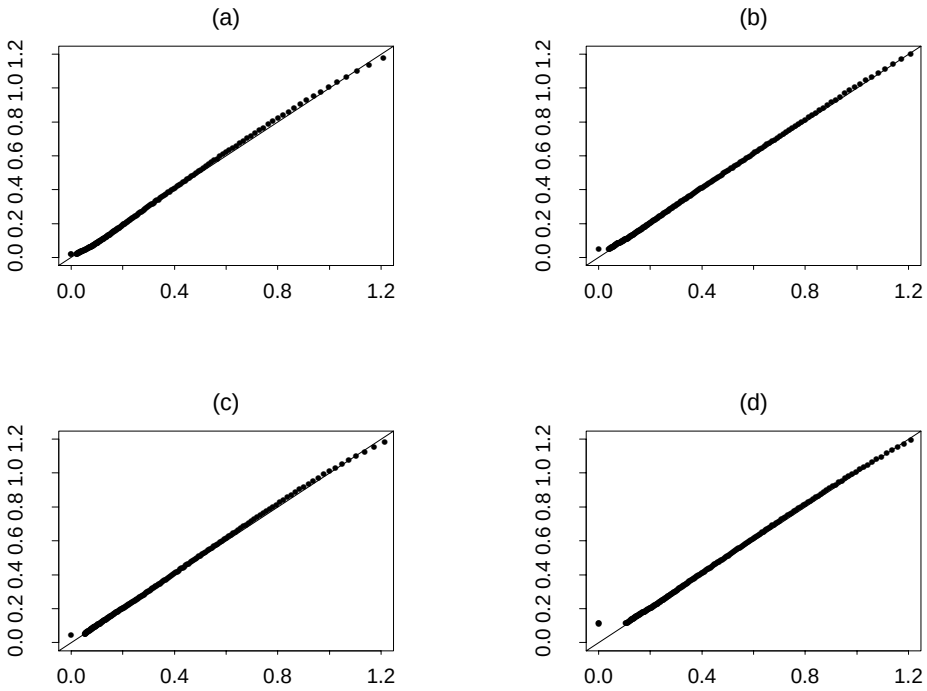

Fig. 9. Plot of $\arcsin((1-\widehat{F}^{km}(r))^{\frac{1}{2}})$ against $\arcsin(\exp(-\pi\hat{\mu}(\frac{2}{3}\hat{R}^3+\hat{R}^2 r)))$ for each experimental group. (a) $\times$5000, short; (b) $\times$5000, long; (c) $\times$7500, short; (d) $\times$7500, long.

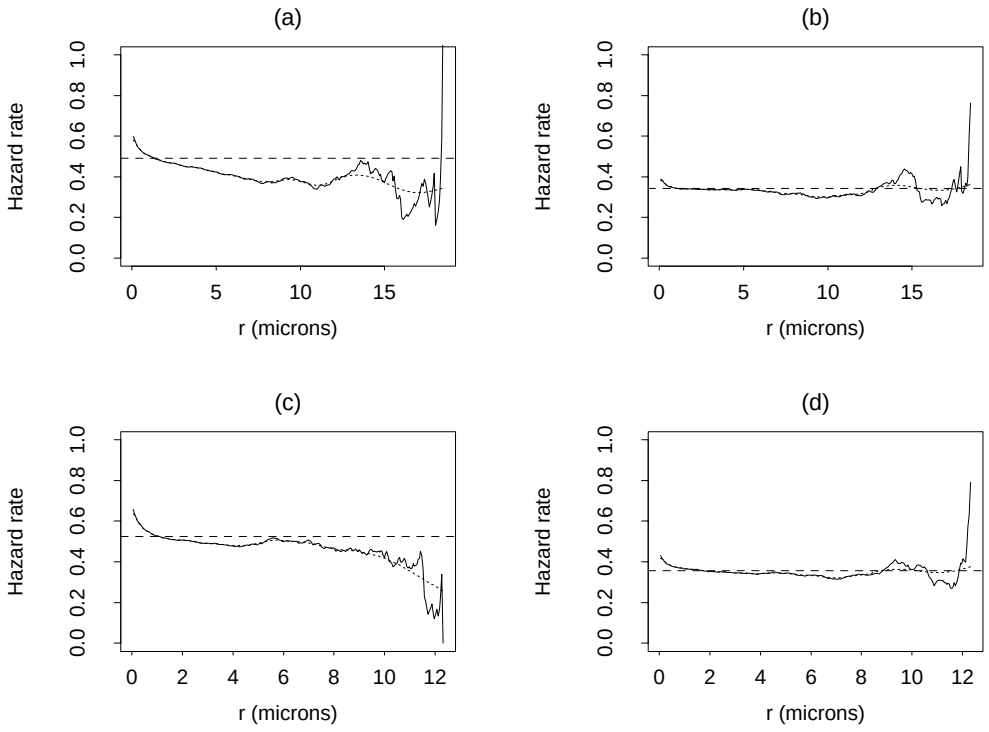

Fig. 10. Estimated linear contact hazard for the pooled estimates shown in Fig. 7. (a) $\times 5000$, short; (b) $\times 5000$, long; (c) $\times 7500$, short; (d) $\times 7500$, long. ——: Point estimate; $\cdots$: Kernel smoothed function, see text; $- - -$: Hazard rate for the estimated Boolean model, see text.

Table 1. *Estimates for the Boolean model, with the jackknife estimates of the standard error given in brackets.*

		short	long
	$\hat{\mu}$	0.2841 (0.0216)	0.1266 (0.0178)
$\times 5000$	$\widehat{R}$	0.5242 (0.0141)	0.6573 (0.0384)
	$\hat{p}_X$	0.1576	0.1400
	$\hat{\mu}$	0.3763 (0.0336)	0.1320 (0.0151)
$\times 7500$	$\widehat{R}$	0.4712 (0.0172)	0.6561 (0.0278)
	$\hat{p}_X$	0.1520	0.1446

Table 2. *Estimates of the star volume, with the jackknife estimate of the standard error given in brackets.*

	short	long
×5000	472.36 (52.55)	1090.36 (107.04)
×7500	316.34 (35.35)	810.51 (63.55)